Human Corneal Fibrosis: An In Vitro Model

Dimitris Karamichos, Xiaoqing Q. Guo, Audrey E. K. Hutcheon, and James D. Zieske

Purpose. Corneal injury may ultimately lead to a scar by way of corneal fibrosis, which is characterized by the presence of myofibroblasts and improper deposition of extracellular matrix (ECM) components. TGF-β1 is known to stimulate overproduction and deposition of ECM components. Previously, an in vitro three-dimensional (3-D) model of a corneal stroma was developed by using primary human corneal fibroblasts (HCFs) stimulated with stable vitamin C (VitC). This model mimics corneal development. The authors postulate that with the addition of TGF-β1, a 3-D corneal scar model can be generated.

Methods. HCFs were grown in four media conditions for 4 or 8 weeks: VitC only; VitC+TGF-β1 for the entire time; VitC+TGF-β1 for 1 week, then VitC only for 3 or 7 weeks; and VitC for 4 weeks, then VitC+TGF-β1 for 4 weeks. Cultures were analyzed with TEM and indirect immunofluorescence.

Results. Compared with the control, addition of TGF-β1 increased construct thickness significantly, with maximum increase in constructs with TGF-β1 present for the entire time—2.1- to 3.2-fold at 4 and 8 weeks, respectively. In all TGF-β-treated cultures, cells became long and flat, numerous filamentous cells were seen, collagen levels increased, and long collagen fibrils were visible. Smooth muscle actin, cellular fibronectin, and type III collagen expression all appeared to increase. Cultures between weeks 4 and 8 showed minimal differences.

Conclusions. Human corneal fibroblasts stimulated by VitC and TGF-β1 appear to generate a model that resembles processes observed in human corneal fibrosis. This model should be useful in examining matrix deposition and assembly in a wound-healing situation. (*Invest Ophthalmol Vis Sci.* 2010;51:1382–1388) DOI:10.1167/iovs.09-3860

One of the critical objectives associated with corneal biology is the understanding of how an organized, dense collagen matrix develops from a population of cells. To be able to even approach this question, we must develop techniques that allow us to understand the underlying mechanisms of collagen production and organization.

In the human cornea, scarring is an inevitable result after trauma, infection, or refractive surgery and can produce blinding complications. Currently, treatment options are limited and consist primarily of corneal transplantation. Pharmacologic intervention is available to slow corneal wound repair; however, it can lead to ulceration rather than prevent scarring.

From The Schepens Eye Research Institute and the Department of Ophthalmology, Harvard Medical School, Boston, Massachusetts.

Supported by National Institutes of Health/National Eye Institute Grant 1R21EY018939.

Submitted for publication April 14, 2009; revised September 15, 2009; accepted October 13, 2009.

Disclosure: **D. Karamichos**, None; **X.Q. Guo**, None; **A.E.K. Hutcheon**, None; **J.D. Zieske**, None

Corresponding author: James D. Zieske, Schepens Eye Research Institute, 20 Staniford Street, Boston, MA 02114; james.zieske@schepens.harvard.edu.

Except for the epithelium, the human cornea exhibits little-to-no regenerative capacity. A mature human corneal stroma is a relatively acellular extracellular matrix (ECM) comprised primarily of hydrated type I/V collagen fibrils (15% wet weight) of uniform diameter (~30–35 nm), glycosaminoglycans (GAGs), keratan and dermatan sulfates, various proteoglycan (PG) core proteins, and miscellaneous other protein constituents, including type VI collagen.[1,2] Stromal function is critically dependent on its nanoscale structure. The major structural collagen of the stroma (type I/V heterotypic collagen—20% type V) is arranged in approximately 250 to 400 lamellae of parallel, non–cross-linked fibrils.[3] The fibrils of adjacent lamellae are nearly perpendicular to each other.

On corneal injury, the keratocytes are stimulated to proliferate (termed fibroblasts) and migrate to the wound site.[4] In some types of wounds, the fibroblasts differentiate further into myofibroblasts and exhibit filaments consisting of smooth muscle actin (SMA). Fibroblasts and myofibroblasts synthesize and secrete a variety of ECM components, including type I and III collagens and fibronectin. When keratocytes are isolated and placed into culture in the presence of serum or growth factors, they become proliferative and then become increasingly quiescent as they reach confluence. Several groups found that the addition of ascorbic acid (vitamin C) increases the proliferative rate of cultured fibroblasts and a loss of contact inhibition.[4–9] In addition, it was reported that vitamin C (VitC) stimulates the synthesis and secretion of ECM components.[5,6,10,11] VitC acts as a cofactor for the enzymes responsible for hydroxylation of the lysine and proline residues on procollagen. These hydroxylations are essential for the stabilization of the interaction of the α chains in the triple helical regions of collagen. This stabilization may allow stratification of cells and accumulation of matrix. Subsequently, it was found that more stable forms of VitC—L-ascorbic acid 2-phosphate and 2-*O*-α-D-glucopyranosyl-L-ascorbic acid—have a far more potent effect on deposition of ECM materials.[5,7,8,12–14] VitC also has been found to stimulate the stratification of several fibroblast types, including dermal[5] and corneal.[7]

Little is known about the growth factors associated with the developmental process; however, the growth factor most commonly associated with corneal fibrosis and fibrosis in general is TGF-β1.[15–22] TGF-β1 has been demonstrated to stimulate the overproduction and deposition of ECM components, such as type I and III collagen,[15–22] as well as, extradomain A fibronectin (EDA-Fn).[23,24] The objective of the present study was to determine whether the stimulation of collagen synthesis by TGF-β1 increases the level of stratification and whether the deposited ECM express fibrotic markers similar to those in corneal scars.

Methods

Primary Culture of Human Corneal Fibroblasts

Primary human corneal fibroblasts (HCFs) were isolated and cultured as previously described in Guo et al.[10] Human corneas were obtained from the National Disease Research Interchange (NDRI, Philadelphia,

Investigative Ophthalmology & Visual Science, March 2010, Vol. 51, No. 3

PA). All research adhered to the tenets of the Declaration of Helsinki. Passages up to number 3 were used throughout the experiments.

Construct Assembly

The HCFs were plated on six-well plates containing polycarbonate membrane inserts with 0.4-μm pores (Transwell; Corning Costar; Charlotte, NC) at a density of 10^6 cells/mL. Fibroblasts were cultured in EMEM with 10% FBS and stimulated by a stable VitC derivative of 0.5 mM 2-*O*-α-D-glucopyranosyl-L-ascorbic acid (Wako Chemicals USA., Richmond, VA). The HCFs were further stimulated with 0.25 ng/mL TGF-β1. Initial experiments examined concentrations ranging from 0.01 to 10 ng/mL. Concentrations of greater than 1 ng/mL caused contraction of the constructs. Four variations of TGF-β1 exposure were examined at 4 and 8 weeks: *Control or C*: The cells were plated on the polycarbonate membranes and cultured with EMEM+FBS+VitC (construct medium). *T1*: The cells were grown in construct medium+TGF-β1 for the entire experiment. *T1–1w*: The cells were grown in construct medium+TGF-β1 for 1 week, at which point, TGF-β1 treatment was removed, and the cells were grown for the remaining 3 or 7 weeks in construct medium only. This experiment was designed to mimic the in vivo wound situation in which the wound-healing epithelium releases TGF-β1 and then levels diminish after epithelial wound closure. *T1–4w*: The cells were grown in construct medium for 4 weeks, at which point, TGF-β1 was added for the remaining 4 weeks of the experiment. At each time point, samples of the resulting constructs were collected and processed for confocal, light, and transmission electron microscopy (TEM).

Confocal Microscopy

The constructs were collected, fixed in 4% paraformaldehyde, and stained for indirect immunofluorescence, as previously described in Zieske et al.[25] After fixation, the constructs were incubated at 4°C overnight with the primary antibodies against type III collagen (Southern Biotech, Birmingham, AL), EDA-Fn (Sigma-Aldrich, St. Louis, MO), SMA (Dako North America, Carpinteria, CA), and Ki67 (Vector Laboratories, Burlingame, CA), in 1% BSA+0.1% Triton-X. The constructs were then washed and incubated overnight at 4°C with the corresponding secondary antibody, donkey anti-goat (type III collagen), anti-mouse IgM (EDA-Fn), anti-mouse IgG (SMA), and anti-rabbit (Ki67; Jackson ImmunoResearch Laboratories; West Grove, PA) in 1% BSA+0.1% Triton-X. Also, a sample of all the constructs was stained with phalloidin (Invitrogen, Carlsbad, CA), which binds to the F-actin in all cells. The phalloidin was conjugated to rhodamine; therefore, no secondary antibody was needed. All constructs were counterstained with iodide (TO-PRO-3; Invitrogen), a marker of all cell nuclei. Constructs were washed, mounted (Vectashield; Vector Laboratories), and observed and photographed with a confocal microscope (TCS-SP2; Leica Microsystems, Bannockburn, IL). Negative controls where the primary antibody was omitted were run with all experiments.

At this time, the construct thicknesses were also measured using the confocal microscope software. Measurements started from the top of the construct (first cell visible) and ended at the bottom of the construct (last cell visible). Thicknesses were analyzed (7–11 samples per condition) for significant difference ($P < 0.05$) using both Student's *t*-test and Dunnett's multiple-comparison test (Prism 5.0; GraphPad Software, La Jolla, CA).

Light and TEM

The constructs were collected, fixed in Karnovsky's fixative (2% paraformaldehyde and 2.5% glutaraldehyde in cacodylate buffer [pH 7.4]) and processed for TEM by using standard procedures as described elsewhere.[26] A diamond knife ultramicrotome (LKB Ultramicrotome, Bromma, Sweden) was used to cut transverse to the plane of the construct. The sections were collected for both light microscopy and TEM. For light microscopy, optical thick sections of 1 to 2 μm were obtained and stained with phenylenediamine and viewed by fluorescence microscope (Eclipse E800 microscope; Nikon, Tokyo, Japan, equipped with a SPOT camera; Diagnostic Instruments, Sterling Heights, MI). For TEM, 60- to 90-Å sections were obtained, viewed, and photographed with a transmission electron microscope (model 410; Philips Electronics NV, Eindhoven, The Netherlands).

Fibril Diameter Measurements

After TEM, photomicrographs of the constructs at the highest magnification (31,000×) were used to measure and quantify the fibril diameter for each condition. Image-analysis software (Photoshop; Adobe Systems, San Jose, CA) was used as a tool. The scale bar for the TEM was used to calibrate the measurements. Ten random fibril diameters were measured for each photo generated. On average, 10 photos were used per condition per time point, resulting in one hundred fibril diameter measurements. Values were then averaged and analyzed for significant variations ($P < 0.05$) with Student's *t*-test and Dunnett's multiple comparison test.

Cell Counting

The total number of cells per construct was determined (Image-Pro Plus, ver. 6.3 software; Media Cybernetics, Bethesda, MD). At least four confocal images per condition per time point were used. The final image stacks from each experiment were split into stacks of 15 images (for example, a stack of 60 images was split into four stacks of 15 images each). Maximum projection was used on those 15 images and processed for automatic cell counting. The number of cells was then calculated for each stack and statistically analyzed for significant variations with Student's *t*-test and Dunnett's multiple-comparison test. An identical process was followed for counting Ki67-positive cells, and the ratio of Ki67-positive cells to total cells was calculated and analyzed.

Results

One of the defining characteristics of fibrosis in all tissues is the excess deposition of matrix materials. Therefore, we initiated our studies with an examination of matrix production. On the addition of TGF-β1, the constructs became thicker. As seen in Figure 1A, the thickness of the construct increased as the exposure time to TGF-β1 increased, at both 4 and 8 weeks. The maximum increase, compared with the control (C: 29.5 and 35.2 μm), occurred when TGF-β1 was added the entire time (T1)—62.2 and 111.8 μm (2.1- and 3.2-fold), 4 and 8 weeks, respectively (Fig. 1A). Of interest, the presence of TGF-β1 for the entire time did not appear to be necessary for the thickness of the construct to increase significantly. A 1-week exposure (T1–1w) resulted in a significant increase in thickness (1.8- and 2.0-fold, 4 and 8 weeks, respectively).

This increase in thickness by TGF-β1 was confirmed when the thick sections of these constructs were compared, as seen in Figure 1B. In all groups, cells stratified, showed a flat and elongated morphology, produced their own collagen matrix, and aligned with and parallel to the porous membrane (Transwell; Corning). Note, that all groups showed high cell densities at the top and bottom of the construct. This area corresponds to where the cells were most highly aligned (data not shown). Of interest, in Figure 1B (T1 at 8 weeks), the cell-produced matrix was losing its integrity. As shown by the white arrow, the collagen at the lower half of the construct was highly disorganized, and the fibrils were mainly running in one direction. In addition, the overall fibril length appeared to decrease, cross-banding became less distinct, and fibril diameter appeared to become more variable. The transition to disorganized matrix was seen at 8 weeks in all T1 samples examined.

Examination of the constructs by TEM revealed the cell-matrix interactions, as well as, matrix condition, such as alignment. Figure 2 shows the constructs after 4 and 8 weeks in culture in all four conditions (C, T1, T1–1w, and T1–4w). The cells appeared elongated and to have produced their own

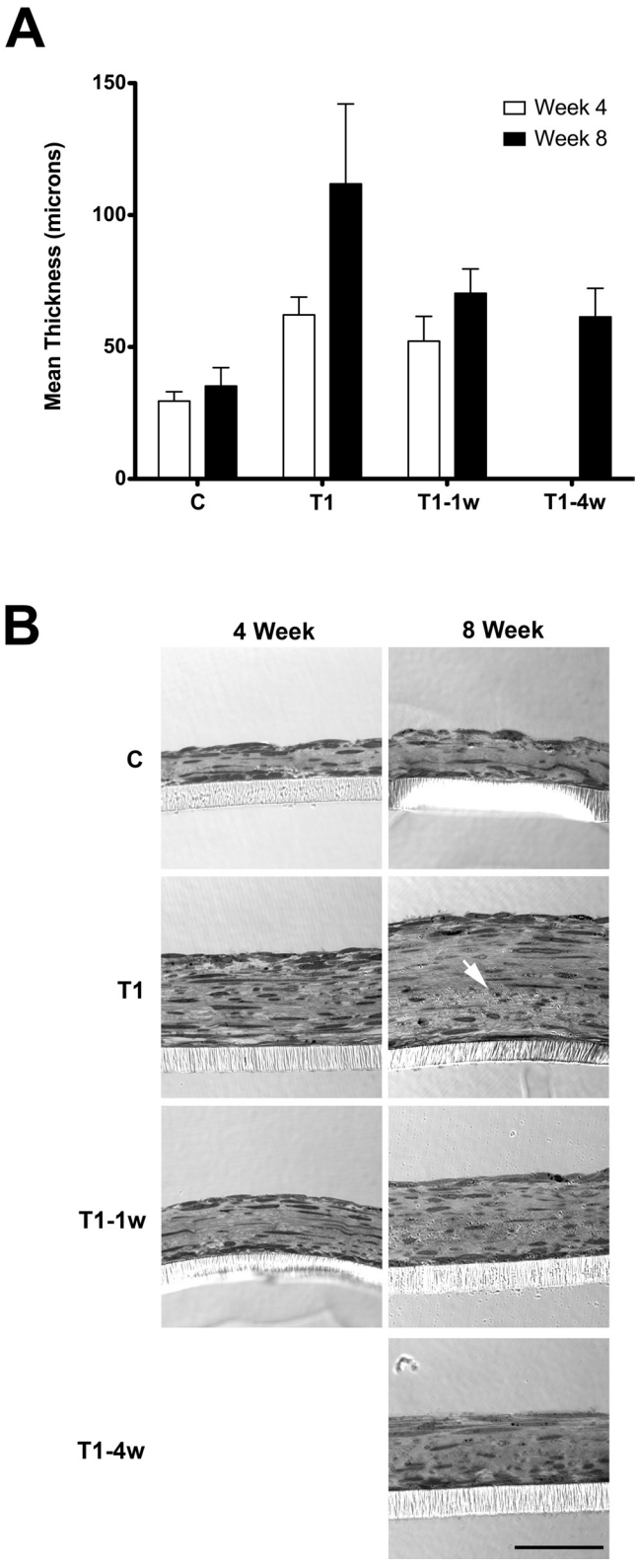

FIGURE 1. (**A**) Construct thickness as measured with the confocal microscope software. T1, T1–1w, and T1–4w are statistically significant compared with C at both 4 and 8 weeks ($P < 0.05$). Week 8 is statistically significant compared with week 4 in each condition ($P < 0.05$). Note that the longer the exposure to TGF-β1, the thicker the construct. (**B**) Optical thick sections of the constructs at 4 and 8 weeks confirm the trend in thickness that was observed with the confocal wholemounts (**A**). Please note that in all constructs, the cells stratified, produced their own matrix, were flat and elongated, and aligned and parallel with the porous membrane. Also, the cell density at the top and bottom of the construct appeared to be higher than in the middle. In T1 week 8, there appeared to be a change in matrix integrity in the area below the *arrow*. Bar, 50 μm.

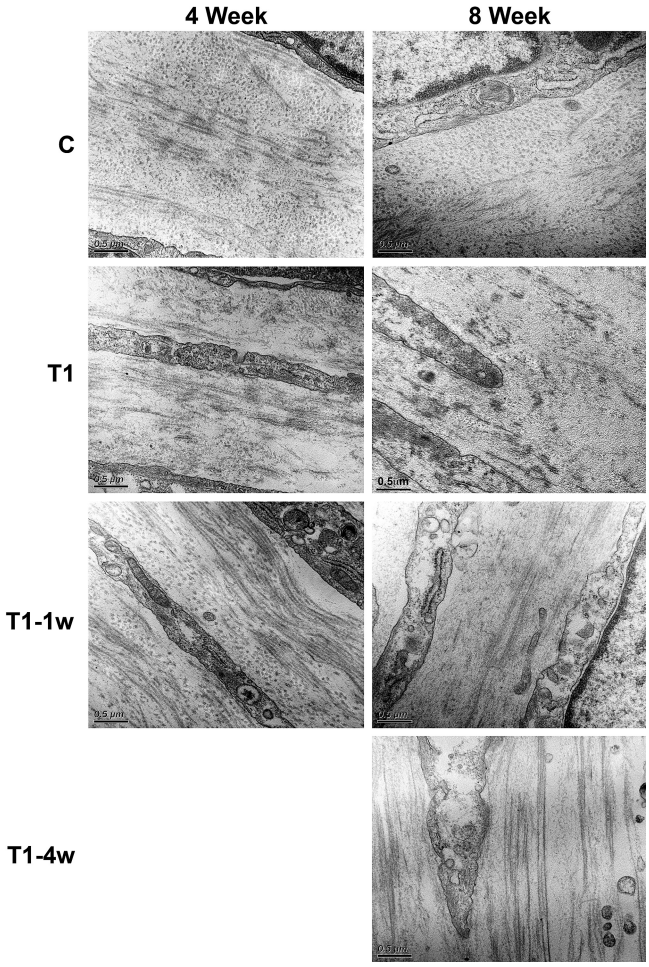

FIGURE 2. High-magnification TEM (31,000×) showing cell–matrix interaction and matrix condition. The fibril orientation changed direction more than once in all the conditions at both 4 and 8 weeks; however, by 8 weeks, T1 fibril integrity appeared to be decreasing. Of interest, at both the 4- and 8-week time points, the fibrils in T1–1w and T1–4w appeared to be longer than those in C. Bar, 0.5 μm.

ECM. Collagen fibril orientation can be identified with several changes in direction in lamellae-like structures. Change of direction and fibril organization is one of the main characteristics of a mature cornea. Our TEM data revealed that the fibrils are organized in C, T1–1w, and T1–4w; however, in T1, the fibrils were shorter and the density of the matrix appeared to decrease by 8 weeks. The fibril length appeared to become longer in T1–1w and T1–4w.

We further quantified and compared the fibril diameters at different conditions, as shown in Figure 3. At 4 weeks, fibril diameters ranged from 30 to 33 μm, sizes comparable to those in vivo (Fig. 3, week 4). Over time, however, the diameter size increased significantly ($P < 0.05$), independent of the presence or absence of TGF-β1 (Fig. 3, week 8, C and T1). Fibril diameter size and integrity were maintained in T1–1w (Fig. 3).

We then investigated the expression of specific fibrotic markers, to assess the cell-produced ECM and to gain an understanding of the effect of TGF-β1. One of these, SMA, marks myofibroblasts, a cell type commonly found in fibrotic tissue.

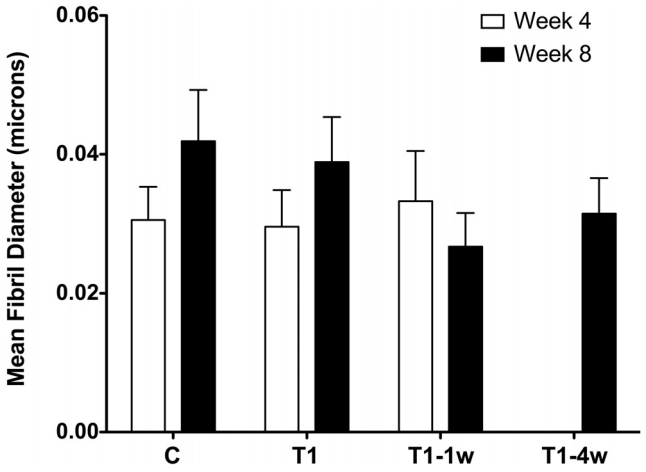

FIGURE 3. Fibril diameter as measured in approximately 10 high-magnification (31,000x) TEM images. Ten fibrils were measured per photo per group and time point. At least 100 fibrils were measured per group. At 4 weeks, the fibril diameter of C, T1, and T1–1w all appeared to be comparable to that in vivo (30–33 μm). Compared with C, T1 is not statistically significant at 4 weeks, whereas, T1–1w versus C is significant ($P < 0.05$). At 8 weeks, the differences observed in C versus T1, T1–1w, and T1–4w are statistically significant ($P < 0.05$). Week 8 is statistically significant compared with week 4 in each condition ($P < 0.05$).

The presence of myofibroblasts and fibrosis are often linked to the production of certain matrix components in the stroma, such as type III collagen and EDA-Fn. As seen in Figure 4 (SMA), few if any myofibroblasts were present in the 4-week construct without TGF-β1 (Fig. 4A; Movie S1, all movies available at http://www.iovs.org/cgi/content/full/51/3/1382/DC1); however, with the addition of TGF-β1 for the entire 4 weeks in culture (Fig. 4B; Movie S2), there was a clear increase in positive SMA cells. These cells were found throughout the construct, but there appeared to be more in the top and bottom layers of the construct. Also, as seen in Figure 4 (Col III), little, if any, type III collagen was present in C (Fig 4C; Movie S3), whereas, in T1, type III collagen was present at a high level (Fig. 4D; Movie S4). Of interest, highest levels of type III collagen appeared in the top half of the construct in TGF-β1-treated cells. EDA-Fn was also upregulated after stimulation with TGF-β1 (Figs. 4E, 4F; Movies S5, S6) and was localized in the topmost layers of the construct. Localization of SMA, EDA-Fn, and type III collagen was very similar between weeks 4 and 8 in all constructs and conditions (data not shown).

The data show that with the addition of TGF-β1, fibrotic markers were upregulated. This finding led us to ask the following questions: For the expression of fibrotic markers, (1) does the construct need TGF-β1 in the construct medium the entire time, and (2) when should the treatment with TGF-β1 take place? Two experiments that mimicked corneal wounding were performed to resolve these questions. As seen in Figure 5, a 1-week pulse of TGF-β1 (T1–1w) increased the number of positive myofibroblasts (Fig. 5A), type III collagen (Fig. 5C), and EDA-Fn (Fig. 5E) compared with the control (Figs. 4A, 4C, 4E). However, the 1-week exposure did not have as much of an effect as the 4-week exposure (T1–4w) seen in Figure 5. As the exposure to TGF-β1 increased, so did the expression of the fibrotic markers—SMA (Fig. 5B), type III collagen (Fig. 5D) and EDA-Fn (Fig. 5F). The localization of fibrotic markers in T1–4w appeared to be close to or similar to that with T1 (Fig. 4). Whereas, the T1–1w construct gave rather intermediate results. There appeared to be no difference between the 4- and 8-week time points for T1–1w (data not shown); therefore, since T1–4w data were collected only at 8 weeks, T1–1w at 8 weeks was used in Figure 5.

Finally, due to the increase in thickness of the constructs, Ki67, a marker of proliferating cells, was used to observe whether there was an increase in proliferating cells on the addition of TGF-β1. In Figure 6, a few proliferating cells were present in C, whereas, in T1, the number of proliferating cells increased considerably. When the percentage of cells expressing Ki67 were quantified (Table 1), it was found that 2.7% and 1.5% of cells in C were positive at 4 and 8 weeks, respectively. In the TGF-β1 treated cells (T1), 3.4% and 1.6% of cells were Ki67-positive. These values were not significantly different. However, when the total number of cells was determined, it was found that C contained 1.6 and 3.0 million cells, 4 and 8 weeks respectively, while T1 contained 3.7 and 6.7 million. These differences were statistically significant ($P < 0.001$). One million cells were originally seeded per construct. No statistically significant difference was recorded in the overall cell density between groups (data not shown).

Overall, it appears that the addition of TGF-β1, even for 1 week (T1–1w), had an effect on the appearance of myofibroblasts and the deposition of both type III collagen and EDA-Fn. As the exposure to TGF-β1 increased so did the effect on the construct. Therefore, there is a direct correlation between the exposure time to TGF-β1 and the expression of fibrotic markers.

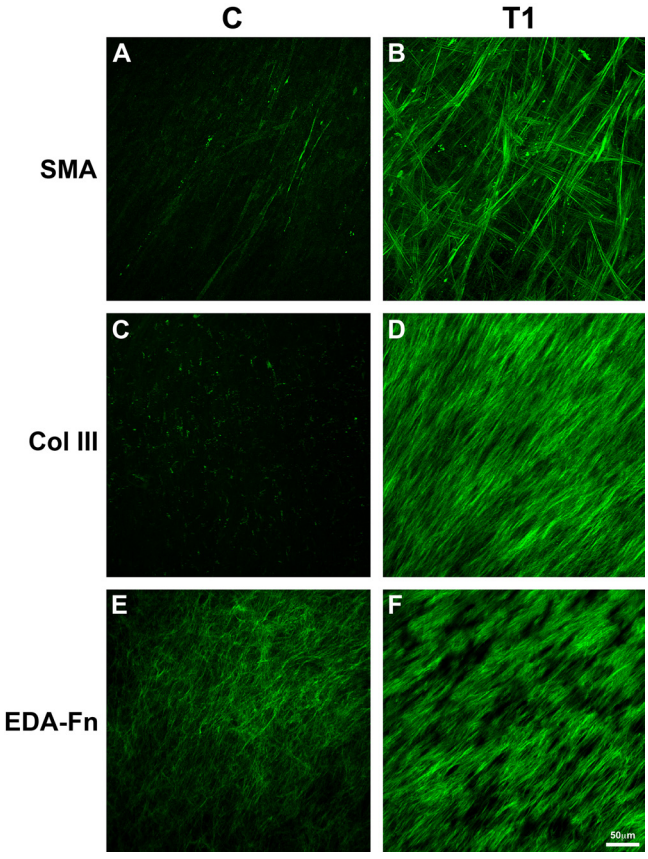

FIGURE 4. Confocal images of full-thickness constructs at 4 weeks. Images show the maximum projection of all the planes of focus for each sample. C or control (No TGF-β1) was compared with T1 (TGF-β1 present for the entire culture time). Fibrosis markers—(**A**, **B**) SMA, (**C**, **D**) type III collagen or Col III, and (**E**, **F**) EDA-Fn—were observed by indirect immunofluorescence. The expression of SMA, type III collagen, and EDA-Fn all increased when TGF-β1 was introduced into the system (T1). Bar, 50 μm.

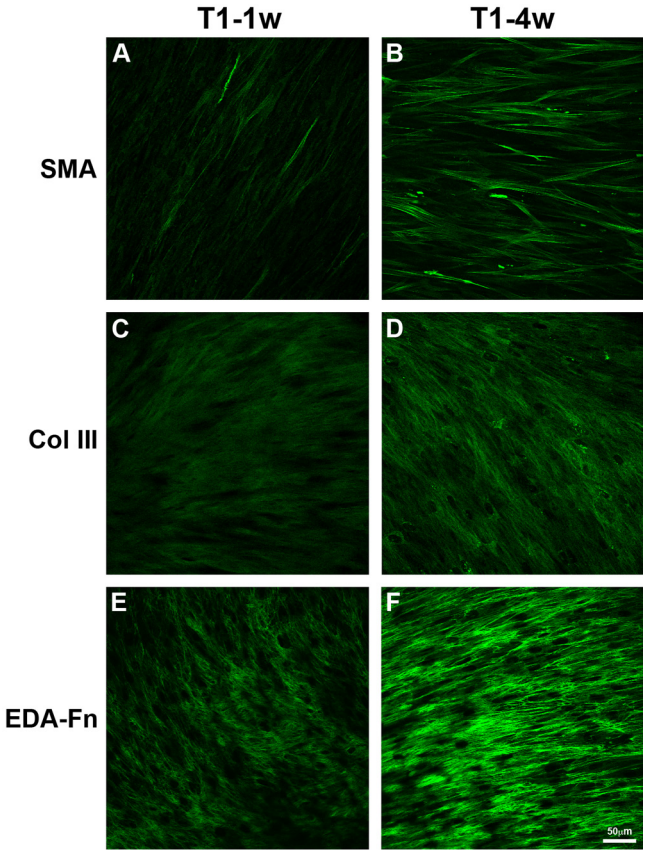

FIGURE 5. Indirect immunofluorescence of fibrotic markers—SMA (**A**, **B**), type III collagen (**C**, **D**), and EDA-Fn (**E**, **F**)—on full-thickness constructs at 8 weeks that were treated with TGF-β1 for various times: T1–1w: TGF-β1 treatment for the first week, then construct medium for the remaining 7 weeks; and T1–4w: construct medium for the first 4 weeks, then TGF-β1 treatment for the remaining 4 weeks. Single plane-of-focus confocal images were selected from the brightest area of immunofluorescence. Four- and 8-week T1–1w constructs appeared to be similar; therefore, since T1–4w was collected only at 8 weeks, we compared T1–1w at 8 weeks. With the addition of TGF-β1 for only 1 week (T1–1w), there appeared to be a slight increase in the fibrotic markers (**A**, **C**, **E**). As the time of TGF-β1 exposure increased (T1–4w), so did the amount of myofibroblasts (**B**), type III collagen (**D**), and EDA-Fn (**F**). Of interest, the point at which TGF-β1 was added to the system (first week or last four) did not seem to be important; however, the length of time TGF-β1 was added to the system appeared to affect the expression of the fibrotic markers. A 1-week treatment appeared to increase the markers, but not to the same extent as the 4-week treatment. Bar, 50 μm.

DISCUSSION

One of the most devastating outcomes of corneal wound repair is the onset of corneal fibrosis leading to scar formation. In contrast to corneal development where copious amounts of collagen fibers are rapidly assembled into a highly organized matrix,[2,27–33] wound repair that leads to a scar involves a mixture of fibroblasts and myofibroblasts,[16,19,34–47] which assemble a disorganized opaque matrix. This matrix is characterized by the presence of fibrotic markers, such as type III collagen, EDA-Fn, and SMA.

In the past, VitC has been found to stimulate the stratification of several fibroblast types, including dermal[5] and corneal.[7] In agreement with these studies, cells in our model stratified to multiple layers in the presence of VitC (control or C). This method of allowing the fibroblasts to assemble their own matrix has been used to engineer tissues, including skin[48] and blood vessels.[49] Previously, we have shown that HCFs stimulated by VitC stratify, secrete, and assemble ECM that mimics the matrix seen during corneal development.[10,11] In this study, we determined whether TGF-β1 treatment of HCFs stimulated with VitC would result in the generation of a scarlike matrix and how this may vary from a normal cornea-like matrix. TGF-β1 has been demonstrated to stimulate the overproduction and deposition of ECM components, such as type I and III collagen,[15–22] as well as EDA-Fn.[23,24] We showed that using our model, ECM components normally present in scars are expressed (i.e., type III collagen and EDA-Fn) and can be turned on and/or off depending on simple timing control. For example, in the T1–1w series, TGF-β1 was added at the beginning and for only 1 week, where the T1 series was exposed to TGF-β1 the whole time. In addition, we examined the structure of the cell-secreted matrix and its level of organization to determine how scar matrix is secreted and organized in a manner different from that in normal cornea. Our data showed a clear difference between the various TGF-β1 stimulations. Overall, our model showed that a scarlike ECM may form with longer exposure to TGF-β1, when compared with no TGF-β1 or a pulselike exposure. Intermediate results were possible, mainly when TGF-β1 exposure was limited to one week. Cells were also able to respond to TGF-β1 after 4 weeks in culture, by producing new ECM, despite the delayed exposure.

Researchers have shown that the ECM components are highly variable. Scars contain high amounts of EDA-Fn and type III collagen, whereas little of either protein is observed during corneal development.[19,23,34,37,38,41–43,46,47,50,51] Hence, our data suggest that the increase in type III collagen and EDA-Fn for the T1-series compared with controls (C) resembles a scarlike ECM formation. In vivo, Jester et al.[20] have demonstrated that treatment of rabbit corneas with TGF-β function-blocking antibodies blunts corneal fibrosis after corneal wounding. Of interest, some matrix was deposited in the presence of the

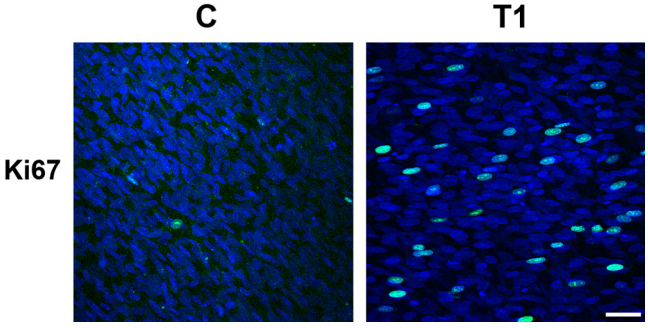

FIGURE 6. Indirect immunofluorescence of proliferation marker, Ki67 (*green*) in full-thickness constructs without (C) and with (T1) TGF-β1 for 4 weeks. Images show the maximum projection of all the planes-of-focus for each sample. *Blue*: iodide, a marker of all cell nuclei. Bar, 50 μm.

TABLE 1. Quantitation of the Positive Ki67 Cells in the Full-Thickness Constructs without (C) and with (T1) TGF-β1

Sample	Week	Avg. Ki67-Positive Cells	Avg. Total Cells	% Ki67-Positive Cells
C	4	43,000	1,600,000	2.68
	8	45,000	3,000,000	1.50
T1	4	128,000	3,700,000	3.45
	8	105,000	6,700,000	1.57

The percentage of positive Ki67 cells is not significantly different; however, the average total number of cells per construct is statistically significant ($P < 0.001$).

anti-TGF-β, suggesting that fibroblasts can be stimulated to secrete matrix in a nonfibrotic manner under the proper conditions. This would correlate with our current T1–1w-series where the cells deposited matrix; however, the ECM components expressed did not completely resemble a scar. It is also interesting to note that the 1-week treatment may mimic a corneal wound where the healing epithelium initially produces high levels of TGF-β1 but then decreases after epithelial wound closure. Data in Figure 5 indicate that the 1-week exposure is sufficient to maintain SMA expression for up to 8 weeks. This result suggests that once the cells are exposed to TGF-β1, they are transformed semipermanently into myofibroblasts. This lengthy transformation also appears to occur in vivo where myofibroblasts are observed years after refractive surgery.

The data presented in this study raise several questions regarding the mechanisms involved in the increase in cell stratification and matrix accumulation associated with TGF-β1 stimulation. It has been known for many years that fibroblasts in culture do not readily convert procollagen to collagen, and subsequently the procollagen is deposited into the culture medium. Musselmann et al.[52] demonstrated that VitC in combination with insulin stimulates the synthesis of collagen and the accumulation of proteoglycans. Of interest, only collagen synthesized in the presence of VitC is pepsin resistant. These authors concluded that VitC stabilizes collagen. We have also demonstrated that fibroblasts cultured in our system synthesize proteoglycans.[11] These proteoglycans were present in both the culture medium and associated with collagen fibrils. The data suggest that stabilization of collagen fibrils by VitC leads to the stratification of the corneal fibroblasts. This hypothesis is supported by the findings of Hassell et al.[53] who found that covering cultures with a layer of agarose leads to increased deposition of matrix and cell stratification. There are several possibilities of how TGF-β1 can lead to increased matrix deposition and cell stratification. The first would simply be that TGF-β1 stimulates more matrix component synthesis leading to more matrix and more cell stratification. A second possibility is that TGF-β1 stabilizes the collagen fibrils produced, thus leading to increased stratification. Finally, it is possible that the altered matrix composition in TGF-β1-treated cells leads to increased stratification. This possibility is supported by the TEM and immunofluorescence data in Figures 2 and 4 (Movies), where the top portions of the constructs expressing highest levels of type III collagen and EDA-Fn were the same areas that in TEM appeared to have the longest fibrils and highest density of matrix.

Conclusion

We have developed an in vitro 3-D model of human corneal stromal cells that allows for the study of cell stratification and matrix assembly that resembles the processes observed in corneal fibrosis.

Acknowledgments

The authors thank Patricia Pearson for technical expertise.

References

1. Meek KM, Leonard DW. Ultrastructure of the corneal stroma: a comparative study. *Biophys J.* 1993;64:273–280.
2. Pouliquen YJ. 1984 Castroviejo lecture: fine structure of the corneal stroma. *Cornea.* 1984;3:168–177.
3. Hamada R, Giraud JP, Graf B, Pouliquen Y. Analytical and statistical study of the lamellae, keratocytes and collagen fibrils of the central region of the normal human cornea (light and electron microscopy) (in French). *Arch Ophtalmol Rev Gen Ophtalmol.* 1972;32:563–570.
4. Zieske JD, Guimaraes SR, Hutcheon AE. Kinetics of keratocyte proliferation in response to epithelial debridement. *Exp Eye Res.* 2001;72:33–39.
5. Hata R, Senoo H. L-ascorbic acid 2-phosphate stimulates collagen accumulation, cell proliferation, and formation of a three-dimensional tissuelike substance by skin fibroblasts. *J Cell Physiol.* 1989;138:8–16.
6. Russell SB, Russell JD, Trupin KM. Collagen synthesis in human fibroblasts: effects of ascorbic acid and regulation by hydrocortisone. *J Cell Physiol.* 1981;109:121–131.
7. Saika S. Ultrastructural effect of L-ascorbic acid 2-phosphate on cultured keratocytes. *Cornea.* 1992;11:439–445.
8. Saika S, Uenoyama K, Hiroi K, Ooshima A. L-ascorbic acid 2-phosphate enhances the production of type I and type III collagen peptides in cultured rabbit keratocytes. *Ophthalmic Res.* 1992;24:68–72.
9. Takamizawa S, Maehata Y, Imai K, Senoo H, Sato S, Hata R. Effects of ascorbic acid and ascorbic acid 2-phosphate, a long-acting vitamin C derivative, on the proliferation and differentiation of human osteoblast-like cells. *Cell Biol Int.* 2004;28:255–265.
10. Guo X, Hutcheon AEK, Melotti SA, Zieske JD, Trinkaus-Randall V, Ruberti JW. Morphologic characterization of organized extracellular matrix deposition by ascorbic acid-stimulated human corneal fibroblasts. *Invest Ophthalmol Vis Sci.* 2007;48:4050–4060.
11. Ren R, Hutcheon AE, Guo XQ, et al. Human primary corneal fibroblasts synthesize and deposit proteoglycans in long-term 3-D cultures. *Dev Dyn.* 2008;237:2705–2715.
12. Kumano Y, Sakamoto T, Egawa M, Tanaka M, Yamamoto I. Enhancing effect of 2-O-alpha-D-glucopyranosyl-L-ascorbic acid, a stable ascorbic acid derivative, on collagen synthesis. *Biol Pharm Bull.* 1998;21:662–666.
13. Nusgens BV, Humbert P, Rougier A, et al. Topically applied vitamin C enhances the mRNA level of collagens I and III, their processing enzymes and tissue inhibitor of matrix metalloproteinase 1 in the human dermis. *J Invest Dermatol.* 2001;116:853–859.
14. Pasonen-Seppanen S, Suhonen TM, Kirjavainen M, et al. Vitamin C enhances differentiation of a continuous keratinocyte cell line (REK) into epidermis with normal stratum corneum ultrastructure and functional permeability barrier. *Histochem Cell Biol.* 2001;116:287–297.
15. Brunet CL, Sharpe PM, Ferguson MW. Inhibition of TGF-beta 3 (but not TGF-beta 1 or TGF-beta 2) activity prevents normal mouse embryonic palate fusion. *Int J Dev Biol.* 1995;39:345–355.
16. Carrington LM, Albon J, Anderson I, Kamma C, Boulton M. Differential regulation of key stages in early corneal wound healing by TGF-beta isoforms and their inhibitors. *Invest Ophthalmol Vis Sci.* 2006;47:1886–1894.
17. Clark RA, McCoy GA, Folkvord JM, McPherson JM. TGF-beta 1 stimulates cultured human fibroblasts to proliferate and produce tissue-like fibroplasia: a fibronectin matrix-dependent event. *J Cell Physiol.* 1997;170:69–80.
18. Faouzi S, Le Bail B, Neaud V, et al. Myofibroblasts are responsible for collagen synthesis in the stroma of human hepatocellular carcinoma: an in vivo and in vitro study. *J Hepatol.* 1999;30:275–284.
19. Ivarsen A, Laurberg T, Møller-Pedersen T. Characterisation of corneal fibrotic wound repair at the LASIK flap margin. *Br J Ophthalmol.* 2003;87:1272–1278.
20. Jester JV, Barry-Lane PA, Petroll WM, Olsen DR, Cavanagh HD. Inhibition of corneal fibrosis by topical application of blocking antibodies to TGF beta in the rabbit. *Cornea.* 1997;16:177–187.
21. Krummel TM, Michna BA, Thomas BL, et al. Transforming growth factor beta (TGF-beta) induces fibrosis in a fetal wound model. *J Pediatr Surg.* 1988;23:647–652.
22. Shah M, Foreman DM, Ferguson MW. Neutralisation of TGF-beta 1 and TGF-beta 2 or exogenous addition of TGF-beta 3 to cutaneous rat wounds reduces scarring. *J Cell Sci.* 1995;108:985–1002.
23. Filenius S, Tervo T, Virtanen I. Production of fibronectin and tenascin isoforms and their role in the adhesion of human immortalized corneal epithelial cells. *Invest Ophthalmol Vis Sci.* 2003;44:3317–3325.

24. Tuori A, Virtanen I, Aine E, Uusitalo H. The expression of tenascin and fibronectin in keratoconus, scarred and normal human cornea. *Graefes Arch Clin Exp Ophthalmol.* 1997;235:222–229.
25. Zieske JD, Hutcheon AE, Guo X, Chung EH, Joyce NC. TGF-beta receptor types I and II are differentially expressed during corneal epithelial wound repair. *Invest Ophthalmol Vis Sci.* 2001;42: 1465–1471.
26. Gipson IK, Grill SM, Spurr SJ, Brennan SJ. Hemidesmosome formation in vitro. *J Cell Biol.* 1983;97:849–857.
27. Cintron C, Covington H, Kublin CL. Morphogenesis of rabbit corneal stroma. *Invest Ophthalmol Vis Sci.* 1983;24:543–556.
28. Hay ED, Revel JP. Fine structure of the developing avian cornea. *Monogr Dev Biol.* 1969;1:1–144.
29. Bard JB, Hay ED. The behavior of fibroblasts from the developing avian cornea: morphology and movement in situ and in vitro. *J Cell Biol.* 1975;67:400–418.
30. Bard JB, Higginson K. Fibroblast-collagen interactions in the formation of the secondary stroma of the chick cornea. *J Cell Biol.* 1977;74:816–827.
31. Birk DE, Trelstad RL. Extracellular compartments in matrix morphogenesis: collagen fibril, bundle, and lamellar formation by corneal fibroblasts. *J Cell Biol.* 1984;99:2024–2033.
32. Chakravarti S, Zhang G, Chervoneva I, Roberts L, Birk DE. Collagen fibril assembly during postnatal development and dysfunctional regulation in the lumican-deficient murine cornea. *Dev Dyn.* 2006; 235:2493–2506.
33. Trelstad RL, Coulombre AJ. Morphogenesis of the collagenous stroma in the chick cornea. *J Cell Biol.* 1971;50:840–858.
34. Bleckmann H, Schnoy N, Kresse H. Electron microscopic and immunohistochemical examination of scarred human cornea retreated by excimer laser. *Graefes Arch Clin Exp Ophthalmol.* 2002;240:271–278.
35. Cintron C, Schneider H, Kublin C. Corneal scar formation. *Exp Eye Res.* 1973;17:251–259.
36. Cintron C, Szamier RB, Hassinger LC, Kublin CL. Scanning electron microscopy of rabbit corneal scars. *Invest Ophthalmol Vis Sci.* 1982;23:50–63.
37. Connon CJ, Marshall J, Patmore AL, Brahma A, Meek KM. Persistent haze and disorganization of anterior stromal collagen appear unrelated following phototherapeutic keratectomy. *J Refract Surg.* 2003;19:323–332.
38. Connon CJ, Meek KM. The structure and swelling of corneal scar tissue in penetrating full-thickness wounds. *Cornea.* 2004;23:165–171.
39. Davison PF, Galbavy EJ. Connective tissue remodeling in corneal and scleral wounds. *Invest Ophthalmol Vis Sci.* 1986;27:1478–1484.
40. Hassell JR, Cintron C, Kublin C, Newsome DA. Proteoglycan changes during restoration of transparency in corneal scars. *Arch Biochem Biophys.* 1983;222:362–369.
41. Ishizaki M, Shimoda M, Wakamatsu K, et al. Stromal fibroblasts are associated with collagen IV in scar tissues of alkali-burned and lacerated corneas. *Curr Eye Res.* 1997;16:339–348.
42. Ivarsen A, Laurberg T, Møller-Pedersen T. Role of keratocyte loss on corneal wound repair after LASIK. *Invest Ophthalmol Vis Sci.* 2004;45:3499–3506.
43. Javier JA, Lee JB, Oliveira HB, Chang JH, Azar DT. Basement membrane and collagen deposition after laser subepithelial keratomileusis and photorefractive keratectomy in the leghorn chick eye. *Arch Ophthalmol.* 2006;124:703–709.
44. Melles GR, Binder PS, Beekhuis WH, et al. Scar tissue orientation in unsutured and sutured corneal wound healing. *Br J Ophthalmol.* 1995;79:760–765.
45. Melles GR, Binder PS, Beekhuis WH, Wijdh RH, Rietveld FJ. Healing of reopened-and-sutured radial keratotomy wounds. *J Cataract Refract Surg.* 1995;21:620–626.
46. Rawe IM, Tuft SJ, Meek KM. Proteoglycan and collagen morphology in superficially scarred rabbit cornea. *Histochem J.* 1992;24: 311–318.
47. Rawe IM, Meek KM, Leonard DW, Takahashi T, Cintron C. Structure of corneal scar tissue: an X-ray diffraction study. *Biophys J.* 1994;67:1743–1748.
48. Auger FA, Pouliot R, Tremblay N, et al. Multistep production of bioengineered skin substitutes: sequential modulation of culture conditions. *In Vitro Cell Dev Biol Anim.* 2000;36:96–103.
49. Berthod F, Germain L, Tremblay N, Auger FA. Extracellular matrix deposition by fibroblasts is necessary to promote capillary-like tube formation in vitro. *J Cell Physiol.* 2006;207:491–498.
50. Ljubimov AV, Alba SA, Burgeson RE, et al. Extracellular matrix changes in human corneas after radial keratotomy. *Exp Eye Res.* 1998;67:265–272.
51. Tervo K, van Setten GB, Beuerman RW, Virtanen I, Tarkkanen A, Tervo T. Expression of tenascin and cellular fibronectin in the rabbit cornea after anterior keratectomy: immunohistochemical study of wound healing dynamics. *Invest Ophthalmol Vis Sci.* 1991;32:2912–2918.
52. Musselmann K, Kane B, Alexandrou B, Hassell JR. Stimulation of collagen synthesis by insulin and proteoglycan accumulation by ascorbate in bovine keratocytes in vitro. *Invest Ophthalmol Vis Sci.* 2006;47:5260–5266.
53. Hassell JR, Kane BP, Etheredge LT, Valkov N, Birk DE. Increased stromal extracellular matrix synthesis and assembly by insulin activated bovine keratocytes cultured under agarose. *Exp Eye Res.* 2008;87:604–611.